

## Chapter 8

## Dispersion and Cavity-Ringdown Spectroscopy

Kevin K. Lehmann

Department of Chemistry, Princeton University, Princeton, NJ 08544

Cavity Ring Down Spectroscopy has become an important method in gas phase spectroscopy and its uses promise to expand. While previous investigators have considered the decay of the stored energy in the cavity ring down cell following short pulsed excitation, this paper considers the effects of pulse reshaping during cavity ring down. It is found that in order to properly model these effects, one must consider not only the mode dependent loss of the ring down cavity, but also dispersion that shifts the resonant modes of the cavity. Only by considering the latter effect does one get a "causal" result where the free induction decay signal of the absorber occurs *after* the excitation pulse. It is demonstrated that in the limit that the cavity round trip time is long compared to both the  $T_2$  time of the intracavity absorber and the temporal width of the excitation pulse, the reshaping of the  $n$ 'th pulse out of the ring down cavity is the same as the reshaping produced by free space propagation over a distance of  $(2n + 1)L$  where  $L$  is the separation of the mirrors in the cell. However, when the absorber  $T_2$  becomes comparable to or longer than the cavity round trip time, then discrete modes of the ring down cavity become important. A general expression for the output is given for the important case of a weak absorber, and changes in the output are computed for a single absorption line as a function of the ratio of  $T_2$  to the cavity round trip time for several values of the optical thickness of the sample. Lastly, it is suggested that monitoring changes in the pulse shape of the cavity ring down signal provides a way to characterize an absorption spectrum on a frequency scale of the laser bandwidth down to the cavity free spectral range.

Cavity ring down spectroscopy (CRDS) has become an important method for obtaining highly sensitive absolute absorption spectra of weak transitions or rarefied species (1-8). Very briefly, CRDS uses pulsed laser excitation of a stable optical cavity formed by two or more highly reflective mirrors. One observes absorption by molecules contained between the mirrors by an increase in the decay rate of photons trapped in the cavity. The absorption spectrum is obtained by measurement of the cavity decay time versus the excitation wavelength. Absorption equivalent noise as low as  $\sim 3 \cdot 10^{-10}/\text{cm} \sqrt{\text{Hz}}$  has been demonstrated, and in principle several orders of magnitude further improvement is possible (3,6).

The theoretical underpinnings of the method have been the subject of recent controversy. O'Keefe (a co-inventor of the method) and his collaborators have favored a "particle" picture of CRDS where one considers the photons injected into the cavity as bouncing incoherently between the cavity mirrors (1,12). Meijer *et al.* (5) noted that a ring down cavity (RDC) is in fact a very high finesse etalon ( $\sim 10^5$  is typical), and considered the effect of the discrete cavity modes on a spectrum observed by CRDS. They pointed out that for a mode matched cavity, one can get distortions in the absorption spectrum due to the filtering produced by the cavity modes of the cell. Zalicki and Zare (9) reach the same conclusion. Meijer *et al.* also pointed out that it is possible to "fill in" the cavity mode spectrum by excitation of high order transverse modes, which are in general shifted in frequency from the TEM<sub>00</sub> modes. However, O'Keefe and collaborators (7) have attacked this conclusion and argued that the complete spectrum of the input pulse enters the ring down cavity when its coherence time is less than the cavity round trip time. They claimed that for short coherence length excitation, CRDS can be completely interpreted by the particle model and that no distortion of the absorption spectrum will occur, regardless of the relative values of the absorption sample's coherence dephasing time  $T_2$  and the cavity round trip time ( $t_r$ ).

This controversy motivated Lehmann and Romanini (10) and Hodges, Looney, and van Zee (11) to develop rigorous theories for the output signal in a CRDS experiment. The only assumptions in these analyses were the most fundamental principles of optics and that of linear absorption by the sample. Further, it was shown that for the important case of a high finesse cavity, the output can be described as a convolution of the input electric field with a Green's function expressed as a sum over all cavity modes, with each cavity mode consisting of a damped exponential times an excitation amplitude that depends upon the spatial properties of the input beam. These results demonstrated that CRDS is only sensitive to sample absorption at the resonant frequencies of excited cavity modes of the RDC, in direct contradiction to the conclusions of Scherer *et al.* (7).

The present paper builds upon that analysis. When the input pulse is shorter than the cavity round trip time, one will always excite more than one cavity mode. Beating of these modes is responsible for the localized traveling wave that moves in the cavity according to the particle model of CRDS. Here we consider changes in the pulse shape as the cavity rings down. If the input radiation pulse width is less than the time it takes light to make one round trip of the cavity but long compared the dephasing time,  $T_2$ , of the absorber, the excitation will create a well defined intracavity pulse that will experience an overall decay in amplitude but otherwise retain the shape of the input pulse. This is the limit where the particle model of CRDS

is appropriate. However, if the sample  $T_2$  is not short compared to the laser coherence time, then the pulse will change shape as it propagates inside the cell, as is well known for the case of free space propagation (13). Such an effect cannot be described by a particle picture since it arises from the selective attenuation and dispersion of the spectral components that make up the intracavity wavepacket. The purpose of this paper is to demonstrate that the mode theory developed by Lehmann and Romanini (10) provides a natural description of this effect. It will be demonstrated that in the limit of a cavity round trip time that is long compared to  $T_2$ , the output of the RDC consists of a series of pulses, each of which is the exactly the same as for free space propagation, such as was previously described by Crisp (13). Comparisons will be made between the free space results and numerical calculations for the case of finite values for the round trip time.

It is important to emphasize that the results presented in this paper are based upon linear response theory and as such are only applicable in the limit of negligible saturation of the sample by the intracavity pulse. The case of intracavity saturation is an important situation since this should allow for sub-Doppler spectroscopy by observation of Lamb Dips when the forward and reverse going pulses interact with the same molecules.

### The Effect of Dispersion on a Mode Matched Ring Down Cavity

Consider a ring down cavity formed by two mirrors with radius of curvature  $R_c$ , separated by a distance  $L$  [which must be  $< 2R_c$  to have a stable cavity (14)]. We define  $t_r = 2L/n_0c$ , the round trip time of the cell, where  $c$  is the speed of light in vacuum and  $n_0$  is the nonresonant index of refraction in the medium between the mirrors. For simplicity, we will assume that the mirrors have identical electric field reflectivity  $\mathcal{R}$  (defined from the substrate side of the mirror, the sign is opposite for reflection from the other side) and transmittivity  $\mathcal{T}$ . The more familiar intensity reflectivity and transmittivity are given by  $R = |\mathcal{R}|^2$  and  $T = |\mathcal{T}|^2$ . Further, we will initially assume that we can treat  $\mathcal{R}$  and  $\mathcal{T}$  as constants over the bandwidth of input radiation to the RDC.

We will assume that the input field is mode matched to the  $TEM_{00}$  transverse mode of the cavity. This is done primarily for mathematical simplicity in that it effectively reduces the problem from three dimensional to one dimensional. Using the general three dimensional results from Ref. (10), the present results can easily be generalized. However, in applications of these results, it is likely that one will want to carefully mode match the radiation. This is because the effects of excitation of multiple transverse modes is to produce a time dependent shape of the cavity output in the plane transverse to the optic axis, due to transverse mode beating. Such effects would likely complicate attempts to study the changes in the pulse shape along the optic axis due to pulse reshaping by the sample. In the ideal case where diffraction losses can be neglected and one detects all the output radiation, there is no interference between different transverse modes due to their orthogonality. In this case, one can just average the cavity output calculated for each set of longitudinal modes associated with fixed transverse mode numbers  $TEM_{mn}$ . In a detailed calculation, one must consider the overlap of the excitation radiation with different  $TEM_{mn}$  modes (10) as well as the shift in resonance frequency with transverse mode numbers.

As demonstrated in Ref. (10) [Eq. (11)], the output of the RDC subjected to arbitrary excitation can be written in terms of a Green's function as:

$$E_o(t) = \int G(t-t')E_i(t')dt' \quad , \quad (1)$$

where  $E_i(t')$  is the electric field of the input radiation, as measured at the input mirror, and  $E_o(t)$  is the electric field of the output radiation, measured at the output mirror. Physically,  $G(t-t')$  gives the output of the cell following a delta function input at time  $t'$ . This simple form of the output is a consequence of the RDC cell being a linear optical system with time independent properties. Under the conditions appropriate for CRDS experiments [see Ref. (10) for details],  $G(t)$  takes the following simple form:

$$G(t) = \frac{1}{\sqrt{2\pi}} \sum_q A(\omega_q) \exp\left(-\frac{t-t_r/2}{2t_d(\omega_q)}\right) \exp[i\omega(t-t_r/2)] \Theta(t-t_r/2) \quad , \quad (2)$$

where  $\omega_q$  and  $A(\omega_q)$  are the angular frequency and excitation amplitude of the  $q$ 'th cavity resonance mode;  $t_d(\omega_q)$  is the ring down time of the  $q$ 'th mode;  $\Theta(t)$  is the unit step function that equals zero for  $t < 0$  and one for  $t \geq 0$ .  $G(t)$  can be calculated from the cavity parameters, the index of refraction,  $n(\omega)$ , and absorption spectrum,  $\alpha(\omega)$ , of the sample inside the cavity by the following relationships:

$$A(\omega_q) = \sqrt{2\pi} \frac{\mathcal{T}^2 e^{-\alpha(\omega)L/2}}{t_r R_{eff}(\omega)} \quad (3a)$$

$$R_{eff}(\omega) = R(\omega) e^{-\alpha(\omega)L} \quad (3b)$$

$$t_d(\omega_q) = \frac{t_r R_{eff}(\omega)}{2[1 - R_{eff}(\omega)]} \quad (3c)$$

The resonance condition for the  $q$ 'th mode is give by:

$$k(\omega_q)L = \pi q + \theta \quad (4)$$

with  $k(\omega) = n(\omega)\omega/c$  the wavenumber of the radiation and  $\theta = \arg(-\mathcal{R})$  the phase shift per reflection from the mirrors. Equation (4) neglects a phase shift due to diffraction (14), which can easily be incorporated into  $\theta$ .

Consider that the RDC is filled with a sample that has a broad band (nonresonant) index of refraction  $n_0$ , and a resonant susceptibility  $\chi(\omega) = \chi' - i\chi''$ , where the sample has a macroscopic polarization defined by  $P(\omega) = \chi(\omega)E(\omega)$ . Since

for a gas the response is isotropic,  $P \parallel E$ , the medium will not change the polarization state of the electric field and we need not consider the vector character of the radiation field. In the presence of an external field, the sample will be anisotropic and the treatment will need to be slightly modified (15). Recently, Meijer's group has reported measurements and theory for polarization selective cavity ring down spectroscopy (16). The field radiated by this polarization leads to both absorption ( $\chi''$ ) and dispersion ( $\chi'$ ). Following Yariv (14) [Eq. (8.2-4)], we can write the index of refraction for small  $|\chi|$  as:

$$n(\omega) = n_0 \left[ 1 + \frac{\chi'(\omega)}{2n_0^2} \right] - i \frac{\chi''(\omega)}{2n_0} \quad (5)$$

From this we see that the absorption coefficient (which describes the exponential decay of the intensity) is given by:

$$\alpha(\omega) = \frac{\omega \chi''(\omega)}{cn_0} \quad (6)$$

The real and imaginary components of  $\chi$  are related by the principle of causality, which insures that the inverse Fourier Transform of  $\chi$  [which gives the Green's function that describes time dependent polarization produced by an impulse  $E(t) = \delta(t)$ ] be zero for all  $t < 0$ . This is traditionally expressed by the Kramers-Kronig relationships, a pair of integral equations relating  $\chi'$  and  $\chi''$ . The traditional derivation of these relationships, which is based upon closing a contour to evaluate the integrals (14) is not valid for a Doppler broadened line, but the classic text by Frohlich (17) presents an alternative derivation that does not have this limitation. Peterson and Knight (18) have presented an efficient Fast Fourier Transform (FFT) method for calculation of the real from the imaginary susceptibility or visa versa.

In order to calculate the cavity resonant frequencies in the presence of the molecular resonance, we substitute Eq. (4) into Eq. (5). Using the fact that  $\chi'$  is small, we can write:

$$\omega_q = \omega_q^0 \left[ 1 - \frac{\chi'(\omega_q)}{2n_0^2} \right] \quad (7)$$

where

$$\omega_q^0 = \frac{2}{t_r} (\pi q + \theta) = \frac{c}{n_0 L} (\pi q + \theta) \quad (8)$$

is the cavity mode condition without sample dispersion. In normal situations, the shift in cavity resonance frequency due to dispersion will be very small. The peak value for  $|\omega_q - \omega_q^0|$  will be about  $\pm 0.3 c \alpha(\omega_0)$  where  $\omega_0$  is the peak of the absorption line (19). Since in CRDS one typically deals with samples where the peak  $\alpha(\omega)$  is  $10^{-5} \text{ cm}^{-1}$  or less, the corresponding shift in resonance modes will be  $|\omega_q - \omega_q^0| < 2\pi \times 10^4 \text{ s}^{-1}$ .

This small shift will be much less than the width of any resonances (20), and thus one can safely replace  $\chi(\omega_q)$  by  $\chi(\omega_q^0)$  in the right hand side of Eqs. (6) and (7). In a traditional CRDS experiment, one filters out all but the slow decay of the light energy in the cell. In this case, since dispersion causes a negligible change in decay rates,  $t_d$ , it has no effect on the CRDS signal, as predicted earlier by Zalicki and Zare (9).

One may wonder if such a small shift could be important at all. Without the contribution from  $\chi$ , the beating of different cavity modes is strictly periodic with period  $t_r$ . The small dispersion contributions cause this periodicity to be lost, and this affects the shape of the pulses leaving the cavity. For example, after a ring down time of  $3.3 \mu\text{s}$ , with  $\alpha(\omega_0) = 10^{-5} \text{ cm}^{-1}$ , light would have traveled one Beer's length through the sample (1 km). Cavity beating terms can be phase shifted by as much as  $\pm 0.5$  radian. This is enough that one may expect to observe significant distortion in the shape of the signal. As the sample becomes even more optically thick, the phase shifts grow proportionally.

Substituting Eqs. (7) and (6) into Eq. (2), and exploiting the approximation that  $R_{\text{eff}} \approx 1$  that was used in the derivation of this equation, it is possible to derive the following expression:

$$G(t) = \frac{\mathcal{T}^2}{t_r} R^{t/t_r - 1/2} \sum_q e^{i\omega_q^0(t-t_r/2)} \exp \left[ -i \frac{\omega_q^0}{2n_0^2} \chi(\omega_q^0)(t-t_r/2) \right] \theta(t-t_r/2) \quad (9)$$

From this equation, using the relationship  $\sum_q \exp(2\pi i q x) = \sum_N \delta(x - N)$ , it is straightforward to show that

$$\lim_{\chi \rightarrow 0} G(t) = \sum_{N=0}^{\infty} \mathcal{T}^2 \mathcal{R}^{2N} \delta(t - t_N) \quad (10)$$

where  $t_N = (N + 1/2) t_r$ , which is the time that the  $N$ 'th pulse would leave the cavity without dispersion. This last result can be derived directly by considering the sum of paths through the cell and thus serves as a check of the present results. Based upon this limit, we expect that even with modest dispersion  $G(t)$  will consist of spikes at times near  $t_N$ , where the different terms in the sum over modes will constructively interfere.

We define a dimensionless time  $\tau = (t - 1/2 t_r)/t_r$ . It is also convenient to add and subtract one to the exponential term in the sum on the right hand side of Eq.(9), since this allows the  $\delta$  function singularity to be treated analytically. This allows the Green's function to be rewritten in the following form:

$$G(t) = \frac{\mathcal{T}^2 \mathcal{R}^{2\tau}}{t_r} \left[ \sum_{N=0}^{\infty} \delta(\tau - N) - \sum_q e^{2\pi i q \tau} \left( 1 - \exp \left[ -i \frac{\pi q + \theta}{n_0^2} \chi(\omega_q^0)(\tau + 1/2) \right] \right) \theta(\tau) \right] \quad (11)$$

The physical interpretation is that, in the limit of a very short optical pulse used to excite the cavity, the sum of  $\delta$  functions is just the external field injected into the RDC, while the second sum represents the field radiated by the absorbers, i.e., the free induction decay (FID) of the sample. For the more realistic case of cavity excitation by a pulse of finite duration, the output is given by the convolution of the input pulse with  $G(\tau)$ . Note that the FID term is in the form a discrete Fourier Transform, and thus the sum can be numerically calculated by a FFT routine (21). If one is considering very short response times, then the assumption of constant  $\mathcal{R}$  and  $\mathcal{T}$  will break down. However, one can generalize the above expressions by explicitly writing  $\mathcal{R}(\omega_q^0)$  and  $\mathcal{T}(\omega_q^0)$  and moving these factors inside the sum over  $q$ .

For a general input electric field, we can use Eq. (1) to calculate the output electric field. However, for the case of an "impulsive" excitation, where the input field is confined to a time much less than the ring down times for the excited modes, this integral becomes a Fourier integral. We are left with the following expression for the output:

$$E_0(\tau) = \mathcal{T}^2 \mathcal{R}^{2\tau} \left[ \sum_{N=0}^{\infty} E_i((\tau - N)t_r) - \frac{\sqrt{2\pi}}{t_r} \sum_q e^{2\pi i q \tau} \left( 1 - \exp \left[ -i \frac{\pi q + \theta}{n_0^2} \chi(\omega_q^0)(\tau + 1/2) \right] \right) \tilde{E}_i(\omega_q^0) \Theta(\tau) \right] \quad (12)$$

where  $\tilde{E}_i(\omega_q^0)$  is the Fourier component of the input wave  $\tilde{E}_i(t)$  at the  $q$ 'th resonance frequency of the cavity. As above, the second sum in the above expression can be efficiently evaluated using an FFT routine.

Let us now consider the special case where the spacing between cavity modes ( $\omega_q^0$ ) is small enough that  $\chi(\omega)$  changes negligibly between modes. This corresponds physically to the situation for which the dephasing time,  $T_2$ , is short compared to the cavity round trip time,  $t_r$ . We expect that the Green's function will be significant only for a few  $T_2$  after the times  $(N + 1/2)t_r$ , i.e.,  $\tau = N$ . In this 'long cell' limit, the sum over modes in Eq. (9) can be replaced by an integral over ( $\omega_q^0$ ), which will just be written as  $\omega$ . Under the approximation that  $R_{\text{eff}} \approx 1$ , this integral expression for  $G(t)$  can be simplified to:

$$G(t) = \sum_N \frac{\mathcal{T}^2 \mathcal{R}^{2N}}{2\pi} \int d\omega e^{i\omega t} \exp \left[ -i\omega \frac{\chi(\omega)}{2n_0^2} t_N \right] \Theta(t - t_r / 2) . \quad (13)$$

Each term in this sum has a natural physical interpretation. Except for the factor reflecting two transmissions and  $2N$  reflections off the cavity mirrors, each term is the Green's function that one gets for free space propagation of the input pulse through the same intracavity medium over a pathlength corresponding to  $(N + 1/2)$  round trips of the cavity (13). Thus in the situation that the absorption dephasing time is short compared to the cavity round trip time (which means that the sample will coherently interact with only one intracavity pulse at a time), the  $N$ 'th output pulse of

the RDC provides a faithful measurement of what the same input pulse would do if it experienced free space propagation over a length  $(2N + 1)L$ .

### Cavity Field with Lorentzian Absorber

An interesting question is how large the ratio  $t_r/T_2$  needs to be for the "long cell" limit to provide an adequate description of the ring down cell output. In this section, we will compare calculated ring down outputs computed for different values of this ratio.

Let us assume that the RDC is filled with a two level Lorentzian absorber, with resonant angular frequency given by  $\omega_0$ , with number density  $N_0$ , and with transition dipole moment given by  $\mu_0$ . We will further assume that all the population is in the lower state of the transition. In this case (14):

$$\chi(\omega) = -\frac{\mu_0^2 N_0}{\epsilon_0 \hbar} \frac{1}{(\omega - \omega_0) - i/T_2} . \quad (14)$$

This sample will have a resonance with frequency full width at half maximum (FWHM) given by  $\Delta\nu = (\pi T_2)^{-1}$  and peak absorption coefficient,  $\alpha(\omega_0)$ , given by:

$$\alpha_0 = \frac{\omega_0 \mu_0^2 T_2 N_0}{c n_0 \epsilon_0 \hbar} . \quad (15)$$

We will now assume that the ring down cavity is excited with a pulse much shorter than  $T_2$ ; we approximate the excitation by a delta function input. In this case, the Green's function directly gives the output signal of the RDC, assuming that  $t = 0$  is defined by the time of cavity excitation. For early times in the ring down ( $\alpha_0 c t \ll 1$ ), the sample will be optically thin for all frequencies. In the long cell limit, we can use Eq. (13) to show that the output is:

$$G(t) = \sum_N \mathcal{T}^2 \mathcal{R}^{2N} \left[ \delta(t - t_N) \frac{c \alpha_0 t_N}{2n_0 T_2} \exp((i\omega_0 - 1/T_2)(t - t_N)) \Theta(t - t_N) \right] . \quad (16)$$

Note that an exponential FID follows each exciting pulse, is out of phase, and builds up in amplitude. For finite values of  $c \alpha_0 t$ , we must consider the effect of the FID acting back on the sample. From the result presented by Crisp (13), it is possible to write an analytic result for this case as well:

$$G(t) = \sum_N \mathcal{T}^2 \mathcal{R}^{2N} \left[ \delta(t - t_N) - \sqrt{\frac{c \alpha_0 t_N}{2n_0 T_2 (t - t_N)}} J_1 \left[ 2 \sqrt{\frac{c \alpha_0 t_N (t - t_N)}{2n_0 T_2}} \right] \exp((i\omega_0 - 1/T_2)(t - t_N)) \Theta(t - t_N) \right] \quad (17)$$

where  $J_1$  is a Bessel function.

We now consider the opposite limit, that of a “short” RDC with  $t_r \ll T_2$ . In this case, at most one cavity mode will strongly overlap the resonant response of the sample. We must now consider the relative position of the resonance frequency and the cavity modes. First, we will consider the case where one of the cavity modes is centered on the resonance,  $\omega_0$ . Referring to Eq. (11), it is clear that the FID will be dominated by the term where  $\omega_q = \omega_0$ . If we only include this term in the sum, the Green’s function can be written as:

$$G(t) = \left[ \sum_N \mathcal{T}^2 \mathcal{R}^{2N} \delta(t - t_N) \right] - \frac{\mathcal{T}^2 |\mathcal{R}|^{2\tau}}{t_r} e^{i\omega_0(t-r/2)} \left[ 1 - \exp\left(-\frac{c\alpha_0}{2n_0} t\right) \right] \Theta(t - t_r/2) \quad (18)$$

$$\xrightarrow{\frac{\alpha_0 c t_r}{\pi T_2} \ll 1} \left[ \sum_N \mathcal{T}^2 \mathcal{R}^{2N} \delta(t - t_N) \right] - \mathcal{T}^2 |\mathcal{R}|^{2\tau} \frac{c\alpha_0}{2n_0} (\tau + 1/2) e^{i\omega_0(t-r/2)}$$

Thus the FID consists of a pure wave at angular frequency  $\omega_0$  whose amplitude starts growing linearly but then saturates. The frequency domain interpretation of this result is as follows: The radiation admitted into the RDC consists of a picket fence of frequencies, only one of which is absorbed by the sample. By the superposition principle, this can be expressed as the picket fence minus a pure wave at  $\omega_0$ . The picket fence corresponds, in the time domain, to a train of delta functions while the pure wave is the FID. This FID saturates once the net wave at the resonance has been completely eliminated. In the time domain approach, we see that having a cavity resonance coincide with the sample resonance insures that the train of delta functions coherently excite the sample, thus the sample coherence and FID grows linearly at first. However, this FID acts to de-excite the sample (since it is out of phase), and we approach a steady state where the two sources of excitation exactly cancel, producing no net absorption. This is related to the area theorem as discussed by Crisp (13).

Now let us consider the case where the sample resonance is exactly half-way between cavity modes  $\omega_q$  and  $\omega_{q+1}$ , while still taking  $t_r \ll T_2$ . The response will be dominated by  $\chi$  at these modes, which will be  $\approx 3$  times larger than for the modes  $\omega_{q-1}$  and  $\omega_{q+2}$ , and thus we make the approximation that only these two modes need be considered. With this approximation, we get:

$$G(t) = \left[ \sum_N \mathcal{T}^2 \mathcal{R}^{2N} \delta(t - t_N) \right] - 2 \frac{\mathcal{T}^2 |\mathcal{R}|^{2\tau}}{t_r} \left[ \cos(\pi\tau) - \cos\left(\left(\pi + \frac{c\alpha_0 t_r^2}{2\pi n_0^3 T_2}\right)\tau\right) \right] e^{i\omega_0(t-r/2)} \quad (19)$$

$$\xrightarrow{\frac{\alpha_0 c t_r}{\pi T_2} \ll 1} \left[ \sum_N \mathcal{T}^2 \mathcal{R}^{2N} \delta(t - t_N) \right] + \mathcal{T}^2 |\mathcal{R}|^{2\tau} \frac{c\alpha_0 t_r}{2n_0^3 \pi T_2} (\tau + 1/2) \left[ \cos(\pi\tau) - \frac{t_r}{\pi T_2} \sin(\pi\tau) \right] e^{i\omega_0(t-r/2)} \quad (20)$$

We thus see that we get an FID wave that is modulated at the cavity free spectral range and has an amplitude that is  $\approx (2t_r/\pi T_2)$  smaller at early times. Including modes further from the resonance line will add higher Fourier components to the FID. Because of smaller  $\chi$  at the cavity modes, the linear approximation works for correspondingly longer times. The leading term, down by one power of the ratio  $t_r/\pi T_2$ , comes from the dispersion contribution to the signal, while the term proportional to  $(t_r/\pi T_2)^2$  arises from the absorption term.

The case of  $t_r \approx T_2$  requires numerical calculation. Figure 1(a) presents the FID amplitude calculated by Eq. (17) for the case of free space propagation at four values of the on-resonance optical depth of the sample,  $(c\alpha_0 t_r)/n_0 = 0.1, 1, 10, 100$ .

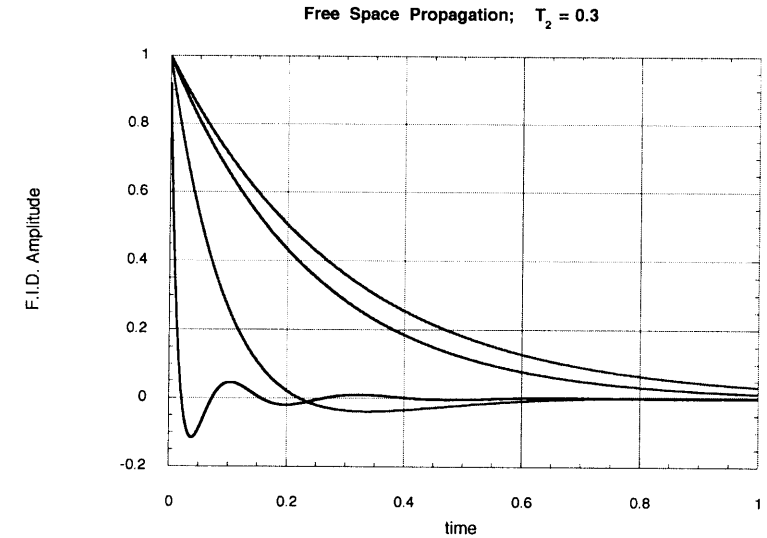


Figure 1a. Normalized Free Induction decay amplitude produced by Free Space Propagation of a  $\delta$  function through a sample with  $T_2 = 0.3t_r$ , where  $t_r$  is the unit of time used in the graph. Calculated by Eq. (17). The Four curves, in order of increasing initial decay rates, are for propagation through a sample with  $\alpha_0 L = 0.1, 1, 10, \text{ and } 100$ , respectively.

The results depend only on the ratio of  $t$  to  $T_2$ , but in order to compare free space and cavity propagation, we have arbitrarily used  $t_r$  as the unit of time for this plot and assumed  $T_2 = 0.3t_r$ . Figure 1(b) presents the FID for the case of a cavity ring down experiment, calculated from Eq. (11), where we have again taken the time unit to be the cavity round trip time  $t_r$ , and the origin equal to  $t_N$ , the output time of the input pulse that travels  $(2N + 1)$  passes of the cavity. The same four values for the on-resonance optical depth are given. The cavity modes were phased so that one mode was exactly resonant with the transition frequency. Despite the fact that the cavity mode spacing is slightly greater than the FWHM of the absorption line, the FID is almost quantitatively the same as for free space propagation over the same path length. The apparent noise near the discontinuity of the FID is an artifact due to the

abrupt cut-off of the high frequency components of the FID, known as the Gibbs' phenomenon (22). These calculations were done using  $2^{10}$  cavity modes with the  $2^9$ 'th mode resonant with the optical transition.

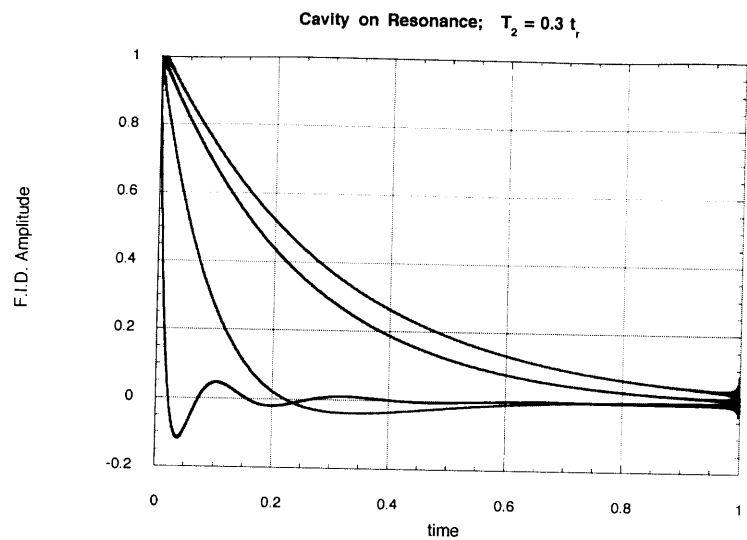


Figure 1b. Normalized Free Induction decay amplitude produced by Cavity Propagation of a  $\delta$  function input through a sample with  $T_2 = 0.3 t_r$ . The time axis is in units of  $t_r$ . The cavity has a resonant mode at the same frequency as the center of the sample absorption line. Calculated by Eq. (11). The Four curves, in order of increasing initial decay rates, are for propagation through a sample with  $c\alpha_0 t_N = 0.1, 1., 10.,$  and  $100,$  respectively.

Figure 1(c) shows the results of the same calculation, but with the optical resonance midway between the  $2^9$ 'th and  $2^9+1$ 'th cavity modes. For high optical depth, the curves are almost identical to the on-resonance case, but for lower optical depths one observes a faster decay and then the FID amplitude goes negative. Figures 2(a-c) presents the results of the same calculation of the free space, on-resonance, and off-resonance calculations, but now with  $T_2 = t_r$ . In this case, the cavity mode spacing is  $\pi$  times greater than the FWHM of the absorption line, and significant deviation from the free space propagation results are evident. What is perhaps remarkable is how similar the on resonance FID remains given the fact that the absorption line is being so dramatically under sampled by the discrete modes of the ring down cavity.

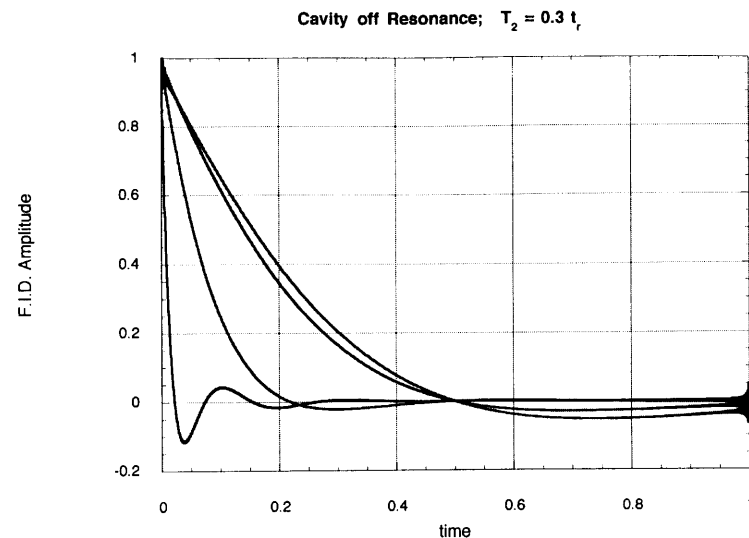


Figure 1c. Same as Fig. 1b except the center of the sample absorption line is exactly half way between two cavity modes.

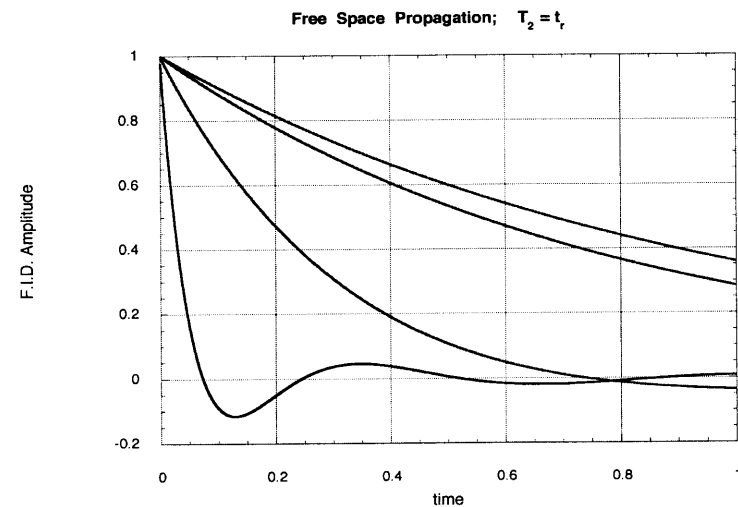


Figure 2a. Same as Fig. 1a, expect with  $T_2 = t_r$ , where  $t_r$  is the unit of time used for the graph.

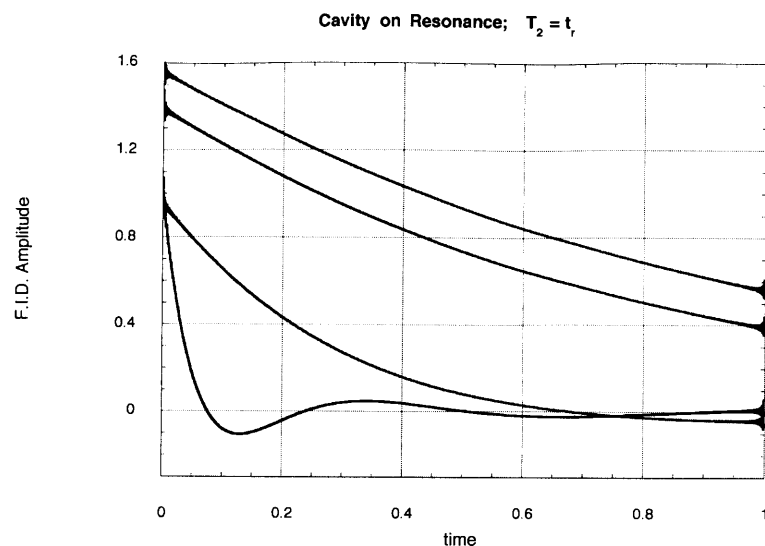


Figure 2b. Same as Fig. 1b, expect with  $T_2 = t_r$ .

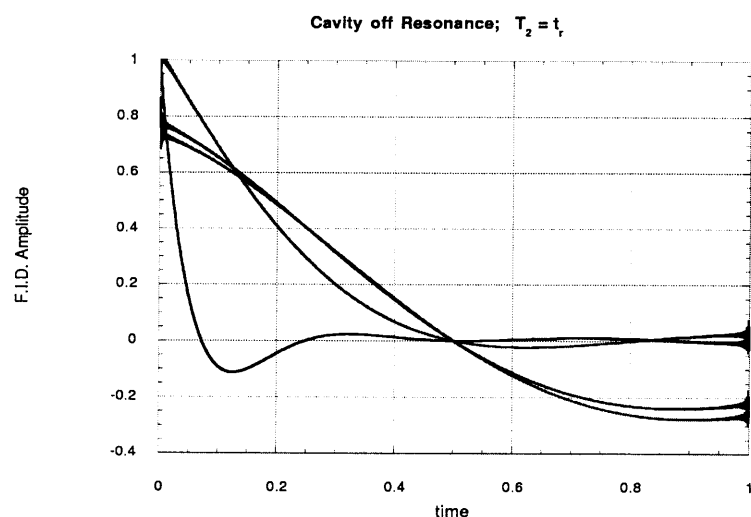


Figure 2c. Same as Fig. 1b, expect with  $T_2 = t_r$ , and the center of the sample absorption line is exactly half way between two cavity modes.

### Cavity Field with Gaussian Absorber

The results presented in the previous section are applicable to the case of a gas phase absorption line with homogeneous width large compared to the Doppler width. For transitions at low to modest pressure, one must include the Doppler broadening of the spectroscopic transitions. The most straightforward way to include Doppler broadening is to convolve the time dependent susceptibility for a Lorentzian line with the inverse FT of the Doppler profile. This assumes that the  $T_2$  time is independent of Doppler shift and also neglects Dicke narrowing effects. This convolution can be evaluated analytically and results in the following expression for the susceptibility:

$$\chi(t) = -i \frac{\sqrt{2\pi} \mu^2 N_0}{\epsilon_0 \hbar} \exp\left(i\omega_0 \cdot t - t/T_2 - \frac{1}{2} \sigma_\omega^2 \cdot t^2\right) \quad (21)$$

where  $\sigma_\omega$  is the standard deviation of the Gaussian Doppler line and is given by:

$$\sigma_\omega = \sqrt{\frac{k_B T}{M} \frac{\omega_0}{c}} \quad (22)$$

In the above expression,  $k_B$  is the Boltzmann constant,  $T$  the sample temperature, and  $M$  the mass of the absorber. Fourier transformation of  $\chi(t)$  gives  $\chi(\omega)$ . The imaginary part of  $\chi(\omega)$  is the Voigt line shape. The real part gives the dispersion of the Voigt line shape. Figure 3 shows the normalized dispersion curve for a line with negligible Lorentzian component. It has the same qualitative shape as for a Lorentzian line shape. Far above and below resonance, it goes to zero as  $\sim 1/(\omega_0 - \omega)$ . It has a minimum and maximum of  $\mp 0.6$  at  $\omega - \omega_0 = \pm 1.3 \sigma_\omega$ . In the wings of the line, the ratio of the dispersive to absorptive line shape is much greater for a Gaussian than for a Lorentzian line shape.

Since in CRDS calculations we are only interested in  $\chi(\omega)$  at the cavity mode frequencies, we can also calculate these by the FFT method. If we wish to calculate modes  $\omega_k$  through  $\omega_{q+N-1}$ , we should compute the FFT of the function  $\exp(-i\omega_q t)\chi(t)$  evaluated at the points  $t_k = k \cdot t_r/N$  with  $k = 0, 1, \dots, N-1$ . Substitution of the resulting  $\chi(\omega_k)$  into Eq. (11) and evaluation by inverse FFT gives the FID decay signal following a delta function input. For a more general input field, the output can be found by substitution of  $\chi(\omega_k)$  into Eq. (12).

### Towards a Time Domain Cavity Ring Down Spectroscopy?

The results of this paper demonstrate that pulse reshaping is a general phenomenon in CRDS whenever the input pulse coherence time is shorter than the dephasing time of the absorbing gas in the cavity. Previous CRDS experiments have not had to consider this effect because the cavity output was strongly filtered to eliminate all but the lowest frequency components of the output intensity. However, we hope the present paper will motivate increased attention to the shorter time characteristics of the output signal since these are sensitive to the sample spectrum over the resolution

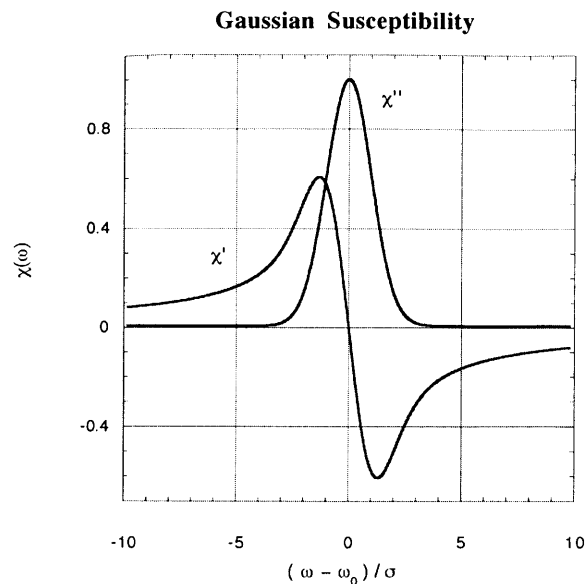


Figure 3. Normalized Real ( $\chi'$ ) and negative Imaginary ( $\chi''$ ) Susceptibility for a Doppler Broadened Transition. Calculated by the Fast Fourier Transform of Eq. (21) with a time step of  $(64\sigma_\omega)^{-1}$  and a total of  $2^{14}$  time steps.

interval between the laser bandwidth and the free spectral range of the RDC. The effect of the resonant modes of the RDC is to replace the continuous Fourier Transform relationship between time and frequency domain response by a discrete Fourier Transform, due to the output field being nearly periodic in time. We have demonstrated that the detailed output pulse shape can be easily calculated from the absorption and dispersion spectra of the sample in the cavity by use of a fast Fourier Transform approach.

These results suggest that it is possible to do CRDS spectroscopy in the “time domain.” We will now demonstrate that such experiments are, at least in principle, practical. To make the discussion more concrete, we will assume that the experiment is designed to detect the concentration and temperature of a molecular oxygen using the A band (i.e., the  $b^1\Sigma_g^+ - X^3\Sigma_u^-$  transition) at  $7620 \text{ \AA}$ . If the sample is assumed to be at room temperature and atmospheric pressure, the individual rotational lines of this band will be pressure broadened to a width of  $\approx 0.1 \text{ cm}^{-1}$  FWHM, which implies  $T_2 \approx 100 \text{ ps}$  (23). Under these conditions, the strong rotational lines have a peak absorption strength of  $\alpha_0 \approx 1 \cdot 10^{-3} \text{ cm}^{-1} \cdot \text{atm}^{-1} \cdot P(\text{O}_2)$ , where  $P(\text{O}_2)$  is the partial pressure of molecular oxygen (23).

Consider the proposed experimental design shown schematically in Fig. 4. A mode locked Ti:sapphire laser with nearly Fourier Transform limited output of  $\Delta t = 5 \text{ ps}$  with repetition period  $\tau_1 \approx 10 \text{ ns}$  is used. With an average power of  $1 \text{ W}$ , this laser will produce output pulses of  $\approx 10 \text{ nW}$  and peak power of  $\approx 2 \text{ kW}$ . Part of this output is amplified in a Regenerative Amplifier, which will be assumed to produce

an output pulse energy  $J \approx 50 \mu\text{J}$ . The output of the amplifier will be mode matched and coupled into a RDC with a nominal length of  $1.5 \text{ meters}$ , producing a cavity round trip time,  $t_r$  only slightly shifted from that of the Ti:sapphire laser. We will further assume that the mirrors of the ring down cavity have  $T = 1 - R = 10^{-4}$ . These conditions that  $\delta t \ll T_2 \ll t_r$  allow one to treat the excitation of the sample as impulsive (i.e., the FID is just proportional to the Green’s function), and the “long cell” limit where the FID’s from different cavity passes do not overlap significantly. In this limit, up to a time where  $A = c \alpha_0 t_n / n_0 \approx 1$ , the intensity of the FID wave leaving the cavity will be:

$$I_{\text{FID}}(t) \approx T^2 R^{2N} A^2 \left( \frac{J \Delta t}{4 T_2^2} \right) \exp[-(t - t_n) / 2 T_2] . \quad (23)$$

$A$  is just the on-resonance absorption of the sample for a pathlength equal to that the light traveled in time  $t_n$ . For  $A \approx 1$ , the output power  $I_{\text{FID}} = 60 \mu\text{W}$  that is  $240 \text{ photons/ps}$ .

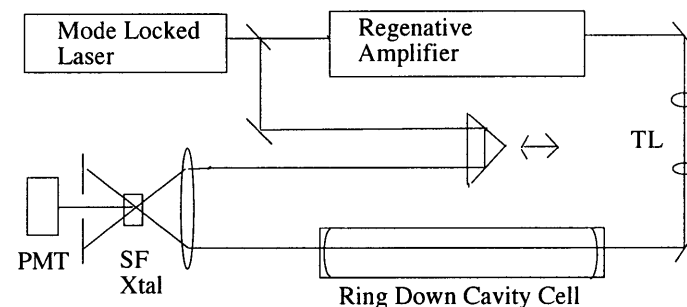


Figure 4. Schematic diagram of experimental apparatus for detection of time resolved Cavity Ring Down Spectroscopy.

This FID intensity will be time resolved by the method of sum frequency generation (SFG), using the light from the oscillator. The FID and pump beam will be assumed to cross at an angle of  $0.1 \text{ rad}$ , which will allow the sum frequency beam to be easily physically separated from the much stronger beam produced by the second harmonic of the pump. We will also assume that we will use Lithium Iodate as the nonlinear crystal. Since the two pulse trains have almost the same frequency, one will “stroboscopically” sweep out the FID, advancing  $\tau_1 - t_r$  each  $\tau_1 \approx 10 \text{ ns}$ . Each such pulse can be resolved and digitized using electronics with a few ns time resolution. If we assume  $\tau_1 - t_r = 10 \text{ ps}$ , we get a time resolution of the FID of  $10 \text{ ps}$  and we sweep out one cycle of the FID curve every  $10 \mu\text{s}$ . Based upon the expressions given by Shah (24), one can calculate a conversion efficiency of  $\approx 0.05$ , thus implying that the peak of the FID will produce  $\approx 300 \text{ SFG photons per oscillator pulse}$ . This is will allow the FID to be obtained with moderate signal to noise even from a single cavity excitation pulse. It should be pointed out that for constant input pulse intensity, the

estimated number of photons scales with the square of the excitation pulse duration ( $\Delta t$ ). Thus, to optimize the FID signal, one should not use an excitation pulse shorter than is needed to resolve the FID signal.

An important practical issue that we have not yet considered is the effect of the finite reflectivity bandwidth of the RDC mirrors. To achieve the shortest possible pulses, one must use specially designed mirrors that have "chirped" coatings (25). The mirrors used in RDCS are designed for maximum reflectivity, which is typically high over a bandwidth of 5–10%. In the red part of the spectrum, these mirrors are made of alternating 1/4 wave layers with indexes of 2.1 and 1.49 (26). Using the transfer matrix method (27), one can calculate the  $\mathcal{R}(\omega)$ . The time dependent output of an impulsively excited RDC cell after  $2n+1$  passes of the cell can be calculated by the Fourier Transform of  $\mathcal{R}(\omega)^{2n}$ . In Fig. 5 is given the calculated output intensity after 10,000 reflections off of a dielectric mirror of 15 pairs of layers, quarter wave at 760 nm. Such a mirror is calculated to have a peak reflectivity of 99.99%.

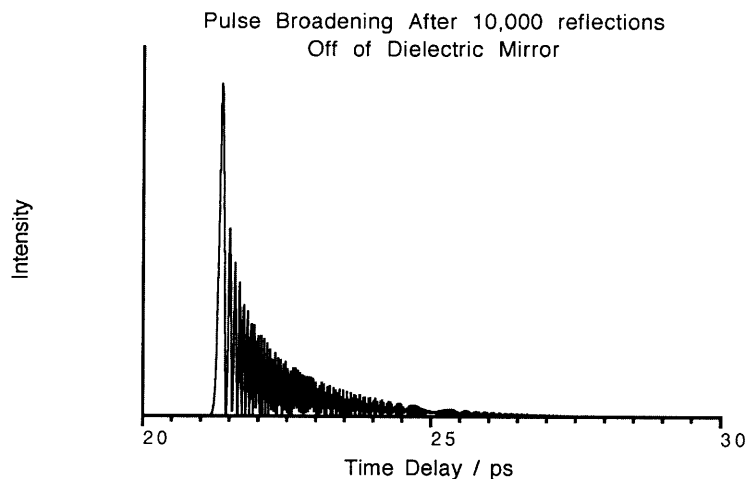


Figure 5. Calculated time dependent intensity of short light pulse after 10,000 reflections off of a high reflectivity dielectric mirror, coated with alternating layers of index 2.1 and 1.49, quarter wave at 800 nm.

The shift in the pulse by  $\approx 22.5$  ps reflects the penetration of the coating by the light, which leads to a slight time delay per reflection, which can be viewed as the cell having a slightly longer effective length. The highly structured decay, with a width of  $\approx 2$  ps reflects the finite bandwidth of the light, filtered by 10,000 reflections. It is thus seen that the finite bandwidth of such a high reflectivity coating will limit one to a time resolution of a few ps.

One must naturally ask if there is any advantage to such a time domain approach to CRDS? In principle, such experiments will not give any information that cannot be obtained by scanning a narrow bandwidth laser over the same spectral region and observing the more traditional frequency domain version of CRDS. The

same objection can be raised against many gas phase, short pulse experiments, and the author acknowledges that he has often found such experiments to be just a needlessly difficult and low signal to noise way of obtaining spectroscopic data. If for no other reason than the current fashion that erroneously views "time domain" experiments as more "direct" than the equivalent frequency domain experiments, the present results will likely find experimental application. Further, there are situations where the time domain approach would offer some practical advantages. The width of a transition can be determined on a single pulse and thus one has a multiplex advantage. This could be useful if one is studying a sample that has an unstable concentration, so that significant noise is observed if a transition is slowly scanned. Another possibility is the study of small spectral widths and splittings, where relatively long FID's could be created and detected with inexpensive lasers and detection equipment, while the equivalent frequency domain experiment may require a highly sophisticated laser to realize the needed resolution. Of course, one must be mindful that the cavity be long enough that the mode filtering not excessively distort the spectral features, but this will be obvious from the observed FID. By off-axis excitation of a cell with a spacing that satisfies the conditions of a Herriott Cell (28), the effective  $t_r$  can be increased to observe even longer FID's.

We conclude that time resolved CRDS, where one observes changes in the intracavity pulse shape as it travels through the sample, is likely to find application in future experiments. The present paper presents the theory needed to interpret and model such experiments.

#### Acknowledgments

The author wishes to thank Dr. Daniele Romanini for a careful reading of this manuscript. I would also like to thank John E. Bertie for pointing out reference 17 and its proof that the Kramers-Kronig relations do hold for a Gaussian line shape. The present work was supported by grants from the New Jersey Commission on Science and Technology and the Petroleum Research Fund, administered by the American Chemical Society. Lastly, I would like to thank the staff of the JILA Scientific Reports Office, who converted my Latex document to a format that is compatible with the ACS choices.

#### Literature Cited

- [1] O'Keefe, A.; Deacon, D.A.G. *Rev. Sci. Instrum.* **1988**, *59*, 2544.
- [2] O'Keefe, A.; Scherer, J. J.; Cooksy, A. L.; Sheeks, R.; Heath, J.; Saykally, R. *J. Chem. Phys. Lett.* **1990**, *172*, 214.
- [3] Romanini, D.; Lehmann, K. K. *J. Chem. Phys.* **1993**, *99*, 6287.
- [4] Yu, T.; Lin, M. C. *J. Am. Chem. Soc.* **1993**, *115*, 4371.
- [5] Meijer, G.; Boogaarts, M. G. H.; Jongma, R. T.; Parker, D. H.; Wodtke, A. M. *Chem. Phys. Lett.* **1994**, *217*, 112.
- [6] Romanin, D.; Lehmann, K. K. *J. Chem. Phys.* **1995**, *102*, 633.
- [7] Scherer, J. J.; Voelkel, D.; Rakestraw, D. J.; Collier, J. B. P. C. P.; Saykally, R. J.; O'Keefe, A. *Chem. Phys. Lett.* **1995**, *245*, 273.

- [8] Zalicki, P.; Ma, Y.; Zare, R. N.; Wahl, E. H.; Dadamio, J.; Owano, T. G.; Kruger, C. H. *Chem. Phys. Lett.* **1995**, 234, 269.
- [9] Zalicki, P.; Zare, R. N. *J. Chem. Phys.* **1995**, 102, 2708.
- [10] Lehmann, K.; Romanini, D. *J. Chem. Phys.* **1996**, 105, 10263.
- [11] Hodges, J. T.; Looney, J. P.; van Zee, R. E. *J. Chem. Phys.* **1996**, 105, 10278.
- [12] Scherer, J. J.; Paul, J. B.; O'Keefe, A.; Saykally, R. J. in *Advances in Metal and Semiconductor Clusters*, **1995**, 3, 149.
- [13] Crisp, M. D. *Phys. Rev. A* **1970**, 1, 1604.
- [14] Yariv, A. *Quantum Electronics*, 3rd ed. (John Wiley, New York, 1989).
- [15] Lehmann, K. K., unpublished.
- [16] Engeln, R.; Berden, G.; van den Berg, E.; Meijer, G. *J. Chem. Phys.* **1997**, 82, 3199.
- [17] Fröhlich, H. *Theory of Dielectrics*, (Oxford, London 1949), section I.2.
- [18] Peterson, C. W.; Knight, B. W. *J. Opt. Soc. Am.* **1973**, 63, 1238.
- [19] For a Gaussian line, the peak value for  $\chi'$  is  $\pm 0.6\chi''$  as shown in section IV. This combined with Eqs (5) and (7) results in this limit.
- [20] Even if there are no other broadening mechanisms, the finite time of flight of a molecule through the TEM<sub>00</sub> beam will result in a broadening of several hundred kHz for typical RDC parameters.
- [21] Press, W. H.; Flannery, B. P.; Teukolsky, S. A.; Vetterling, W. T. *Numerical Recipes* (Cambridge University Press, Cambridge, 1989).
- [22] Gibbs, J. W. *Nature*, **1899**, 59, 606.
- [23] Ritter, K. J.; Wilkerson, T. D. *J. Mol. Spectrosc.* **1987**, 121, 1.
- [24] Shah, J. *IEEE J. Quantum Electronics* **1988**, 24, 276, Eq. (14).
- [25] Mayer, E. J.; J. Möbius, J.; Euteneuer, A.; Rühle, W. W.; Szpöcs, R. *Opt. Lett.* **1997**, 22, 528.
- [26] Lalezari, R. *Research Electro-Optic*, private communication.
- [27] Fowles, G. R. *Introduction to Modern Optics*, 2nd ed. (Dover, New York 1975). See in particular Eq. (4.30).
- [28] Herriott, D.; Kogelnik, H.; Kompfner, R. *Appl. Opt.* **1964**, 3, 523.

## Cavity-Ringdown Spectroscopy versus Intra-Cavity Laser Absorption

Daniele Romanini

**Laboratoire de Spectrométrie Physique—CNRS UMR 5588, Université  
J. Fourier de Grenoble, B. P. 87—38402 Saint Martin d'Hères Cedex, France**

Cavity ring down spectroscopy (CRDS) and intra cavity laser absorption spectroscopy (ICLAS) are among the most powerful quantitative absorption methods. In view of the growing interest they attract, we will give a detailed comparative description of their most relevant features. We will try considering all recent developments, for example the use of continuous lasers or of single mode pulsed lasers in CRDS, and the single-pulse ICLAS by correlated double sampling. These are rather complementary methods, and the choice of the most appropriate will vary with the applications. Among these, most promising are trace detection and high resolution spectroscopy of transient species in plasmas or supersonic jets.

In spectroscopy, high sensitivity absorption is used extensively for the characterization of extremely weak transitions. For example, the investigation of highly excited vibrational (overtone) states has contributed to much of the current understanding of molecular dynamics. In astrophysics, weak transitions characterize the solar spectrum filtered through the atmospheres of the sun and of the earth, and for more distant stars, their spectra may collect information about diffuse interstellar clouds. This precious information about very remote environments can be decoded only after identification and spectral characterization of the carriers of those weak transitions in controlled laboratory conditions.

In the future, compact spectroscopic devices allowing ultrasensitive, selective, and quantitative absorption measurements will be an indispensable aid in trace detection and environmental monitoring, which range from urban pollution to security of industrial sites, from semiconductors processing to medicine and agronomy. In general, spectroscopic methods based on direct absorption offer a quantitative measurement of the absorption coefficient, which is the product of the concentration and the (temperature dependent) integrated cross section of